



A NOVEL APPROACH FOR CONTROLLING WITH A MATRIX CONVERTER

BOUROUNECH CHARAF¹, LEHOUCHE HOCINE², MENDIL BOUBEKEUR³

Keywords: Matrix converter; Venturini method; Lyapunov's functions.

This paper presents the contribution of a matrix converter for frequency stabilization for an energy source. Venturini optimal amplitude method is used. The energy source frequency is assumed to be purely random. A new approach based on the concept of Lyapunov's functions is revealed. The study is done for an electrical network with a random variable frequency, following the normal distribution and a typical RL load. The approach is tested using simulations under MATLAB® /Simulink® environment. The criteria used in the analysis are signal form, frequency analysis, and THD. The performances obtained are discussed.

1. INTRODUCTION

Two control strategies of matrix converter (MC) are mainly adopted. The first is based on spatial vector modulation SVM [1–3]. The second is analytic based on the Venturini optimum amplitude method. The main advantage of the SVM method is that the losses at the switch levels are lower than the method of Venturini. But the latter offers better performances on the harmonics [4].

The MC was introduced in 1976 [5]. Then, its first mathematical form was formulated in 1980 by Venturini and Alesina [6] and was named Matrix Converter. In 1989, Venturini and Alesina proposed the optimum amplitude method [7]. The latter was appreciated and continues to gain a growing interest.

The MC has been studied intensely as an alternative to conventional indirect power converter systems because of its outstanding advantages [8]: sinusoidal input and output currents with minimum harmonics, absence of reactive elements in direct current, adjustable displacement factor for any load, operational in the four quadrants, simple and compact design. These properties have motivated researchers to study the MC [9–11].

On the other hand, the use of the MC remains limited in the face of constraints such as a source of energy being unstable in frequency and/or amplitude, the connection of a power source, or the input phases being asymmetrical. The load needs to be more, *etc.* Any distortion at the source is transmitted directly to the load due to the absence of an intermediate dc circuit. The frequency variations are due to several causes, such as random frequency around 50 Hz with small variations due to consumption dynamics, strong local variations occurring during incidents such as short-circuits, or overall frequency variations caused by abrupt changes in production.

However, many studies have yet to be done to raise the challenges of MC. In Patel [12], the performance of MC is verified by connecting a 3-phase induction motor. In [13], Rodriguez implemented the optimal modulation of Venturini and showed a greater relationship between magnitudes of the input and output voltages of an MC (3X4), which can work with load balanced or unbalanced. In Boukadoum [14], implementing the Venturini optimal method with fuzzy logic significantly reduces ac/ac conversion harmonics applied to a disturbed input voltage. Chaoui in [15], obtained results that show the efficiency of

the FLC type 2 with the Venturini method by offsetting the big uncertainties. Karaca [16] developed an algorithm for a closed-loop compensation based on Venturini optimal method and the FLC approach. It can be easily adapted to the MC. The study was performed for distorted input voltage conditions and all output frequencies from 10 Hz to 100 Hz. The proposed method reduced the input and output harmonics' content and allowed load current control. In [17], a design and validation of an MC driving a motor, tubular, linear, permanent magnet, high force density, is presented.

This work presents new control law with an MC using Venturini optimal amplitude method. It's based on the Lyapunov function approach. The study assumes an energy source passes through a time phase of frequency instability. Simulation results are evaluated based on state space signal forms, frequency analysis, and THD calculation criteria.

This paper is organized as follows. After this introduction, section 2 presents the mathematical modelling of the system. The Venturini method is described considering perfect switches. Section 3 is dedicated to the new control approach. The simulations and discussion are presented in section 4 Section 5 concludes this paper.

2. MATHEMATICAL MODELLING

MC is an ac/ac power converter with bidirectional power switches ($m \times n$). Each switch comprises two IGBTs and two fast diodes connected in antiparallel. The basic topology of an MC connects a three-phase of a voltage source ($m = 3$) to a three-phase load ($n = 3$) which is represented in Fig. 1. This is the most important MC topology from a practical viewpoint.

The principle is that the MC synthesizes the desired three-phase output voltages from the input ones for each well-defined switching period. In this case, the output voltage is formed, in each switching period, by segments of the three input voltages, while segments of the three output currents form the input current. The supply network was idealized during the modeling, and the input filter was omitted. Similarly, some considerations have been made for the switches to be ideal.

^{1,2,3} Department of Electrical Engineering, Mira A. university, Bejaia, Algeria, E_mail: ¹ Bourounechcharaf@yahoo.fr,

² Lehouche2006@yahoo.fr, ³ bmendil@yahoo.fr

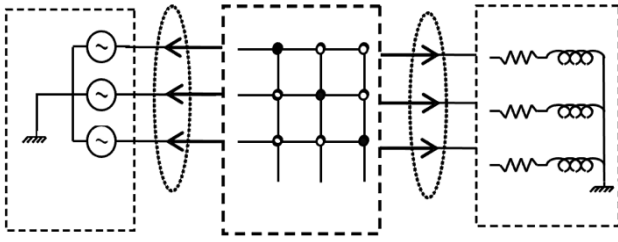


Fig. 1 – Basic topology of a matrix Converter (MC).

Each switch is characterized by a switching function, defined by (01) and can connect or disconnect phase K from the input stage to phase j of the load

$$S_{kj} = \begin{cases} 0 & \text{open switch} \\ 1 & \text{closed switch} \end{cases} \quad (1)$$

$$k = \{A, B, C\}, j = \{a, b, c\}$$

Table 1
Symbol designation

Designation	Symbol
Input voltage	V_e
Input current	I_e
Load voltage	V_{jN}
Load current	I_c
Activation time of the switch	t_{kj}
Sampling interval	T_s

Output voltages, V_{jN} can be synthesized by input voltages for each combination appropriate to the switches.

The control laws must respect two basic rules.

1. Two input phases must never be connected to prevent short-circuits.
2. An output phase must always be connected to avoid surges while the load is inductive.

These two constraints can be expressed by:

$$\sum_{k=A,B,C} S_{ka}(t) = \sum_{k=A,B,C} S_{kb}(t) = \sum_{k=A,B,C} S_{kc}(t) = 1. \quad (2)$$

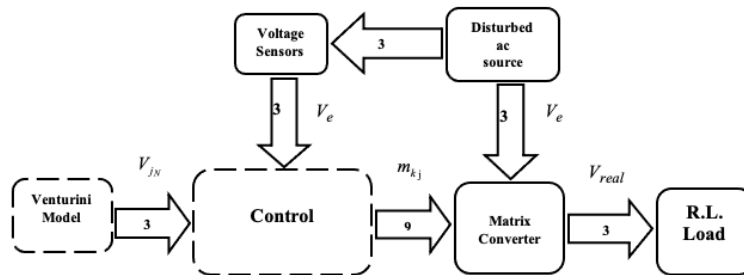


Fig. 4 – Control block.

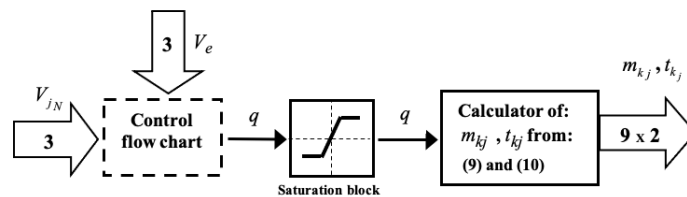


Fig. 3 – Synoptic scheme for an MC control.

frequencies to the target output phase voltage, as shown in (8).

Applying these two rules for 512 ($=2^9$) possible combinations, we have only 27 qualified combinations.

If t_{kj} is defined as the time during which switch S_{kj} is on, and T_s the sampling interval, the duty cycle of switch S_{kj} can be given as follows:

$$m_{kj} = \frac{t_{kj}}{T_s}. \quad (3)$$

So, modulation matrix can be given as in (4).

$$M(t) = \begin{bmatrix} m_{Aa} & m_{Ba} & m_{Ca} \\ m_{Ab} & m_{Bb} & m_{Cb} \\ m_{Ac} & m_{Bc} & m_{Cc} \end{bmatrix}. \quad (4)$$

Under ideal input voltage conditions, the three-phase sinusoidal input voltages of the MC will be as follows:

$$V_e(t) = V_{im} \begin{bmatrix} \cos \omega_i t \\ \cos(\omega_i t + 2\frac{\pi}{3}) \\ \cos(\omega_i t + 4\frac{\pi}{3}) \end{bmatrix}. \quad (5)$$

In accordance with this, each output phase voltages can be expressed by (6).

$$V_{jN}(t) = M(t)V_{e_k}(t). \quad (6)$$

In the same way, the input currents are also shown by the following expression.

$$I_e(t) = M^T(t)I_{jN}(t). \quad (7)$$

where, $M^T(t)$ is the transpose matrix of $M(t)$.

The output voltage amplitude is limited to 50 percent of the input voltage in the initial approach of the Venturini method. To obtain a maximum voltage transfer ratio, added third harmonic of the input and output.

$$V_{j_N}(t) = qV_{im} \begin{cases} \cos \omega_o t - \frac{\cos 3\omega_o t}{6} + \frac{\cos 3\omega_i t}{2\sqrt{3}} \\ \cos(\omega_o t + \frac{2\pi}{3}) - \frac{\cos 3\omega_o t}{6} + \frac{\cos 3\omega_i t}{2\sqrt{3}} \\ \cos(\omega_o t + \frac{4\pi}{3}) - \frac{\cos 3\omega_o t}{6} + \frac{\cos 3\omega_i t}{2\sqrt{3}} \end{cases} \quad (8)$$

where q is the voltage gain or voltage transfer ratio. This way, a voltage transfer ratio of 0.866 in the Venturini optimal amplitude, which is the maximum value, can be obtained.

The algorithm can be simpler if a unity input displacement factor is required (9).

$$m_{k_j} = \frac{1}{3} + \frac{2V_{e_k} V_{j_N}}{3V_{im}^2} + \frac{2q}{9q_m} \sin(\omega_i t + \beta_k) \sin 3\omega_i t \quad (9)$$

$$k = \{A, B, C\}, j = \{a, b, c\}, \beta_k = \left\{0, \frac{2\pi}{3}, \frac{4\pi}{3}\right\}$$

Then, duty cycles of bidirectional switches are calculated according to (10).

$$t_{k_j} = T_s \left(\frac{1}{3} + \frac{2V_{e_k} V_{j_N}}{3V_{im}^2} + \frac{2q}{9q_m} \sin(\omega_i t + \beta_k) \sin 3\omega_i t \right). \quad (10)$$

Finally, the boot of the nine switches of the MC is obtained using a simple binary logic.

$$X = t_{A_j}, \quad Y = t_{A_j} + t_{B_j}. \quad (11)$$

which implies in (12) and illustrated by a Fig. 2.

$$S_{A_j} = (X), \quad S_{B_j} = (\overline{X}) \wedge (Y), \quad S_{C_j} = (\overline{X}) \wedge (\overline{Y}). \quad (12)$$

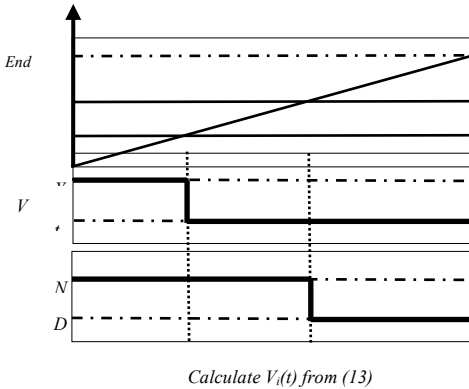


Fig. 2 – Generation of gate signal for switches.

2. CONTROL SYSTEM.

Under the conditions of a voltage source crossing a phase of unstable frequency, the use of fixed switching models is unsuitable. Therefore, the duty cycles for the switching models must be calculated instantly by measuring the output voltages at each sampling period. In this context, we present a new approach when we clarify.

An MC form a class of hybrid systems; the general model includes many subsystems. The particularity that these are linear.

The concept of stability is closely related to the theory of stability in the sense of Lyapunov [18]. This theory establishes that systems whose trajectory is attracted to an asymptotically stable equilibrium point lose energy gradually and monotonously.

Lyapunov generalizes the notion of energy as a function $V(x)$ which depends on the system's state. In this context, several studies have been devoted to answering stabilization and control questions with the concept of Lyapunov [19–25]. For that, we propose the following common quadratic Lyapunov function:

$$V_i(t) = \Delta_i^{tr}(t) \frac{I_3}{2} \Delta_i(t). \quad (13)$$

$$\Delta_i(t) = S_{k_j}(i)V_e(t) - V_{j_N}(t) \quad (14)$$

$k = \{A, B, C\}, j = \{a, b, c\}, i = 1, 2, \dots, 27.$

I_3 : Identity Matrix of order 3.

$\Delta_i^{tr}(t)$ is the transpose of $\Delta(t)$.

The chosen subsystem is that the common quadratic Lyapunov function is closer to zero.

Figure 3 shows the synoptic diagram of the system. We have a disturbed voltage source at the input of the MC, so we have voltage sensitive sensor.

After processing according to our proposed method, a control block instantly receives both the voltage measurements taken by the sensors and the voltage model according to the Venturini method; the MC then receives signals suitable for the switches. Figure 4 gives more detail on the control block.

First, we have a sub-block with a control flowchart that calculates at each commutation the value of the gain q , then a sub-block of saturation function is inserted whose usefulness is to limit the gain between 0 and 0.866. Lastly, a block generates the activation signals suitable for the MC switches.

Figure 5 presents a control flowchart for this proposed strategy.

- At startup, the system parameters are assigned, then at each switching period, the following operations are performed:
- Part 1: Calculations from the first iteration are considered as a benchmark.
- Part 2: Starting at the second iteration, the evaluation of the common Lyapunov function is carried out for all 27 authorized subsystems in an iterative order. On the other hand, the mode that achieves the pursuit's objective is selected at the last iteration.
- Part 3: The Venturini model is used. The voltage gain q is calculated according to eq. (8).

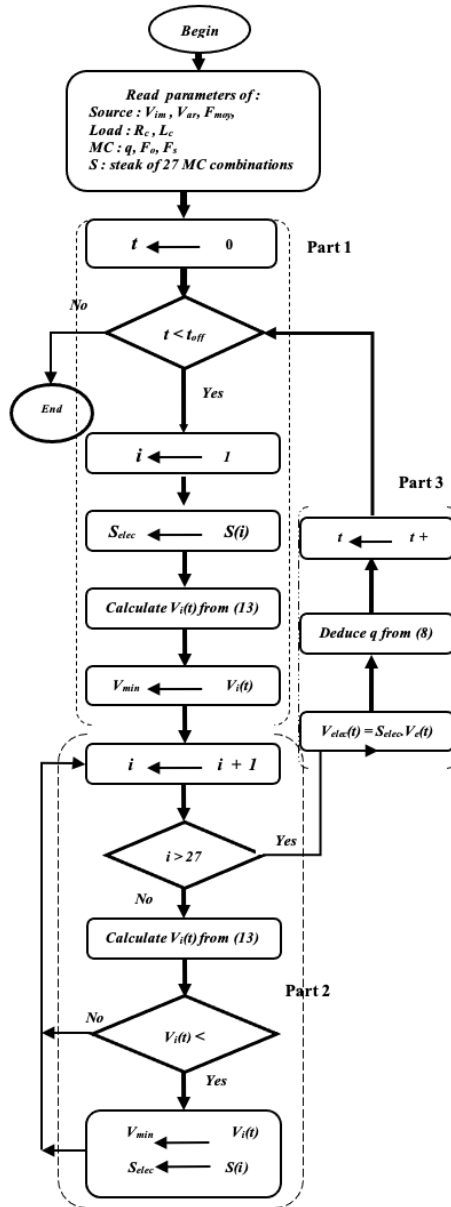


Fig. 5 – Control flowchart

3. SIMULATIONS AND DISCUSSION

Simulations are performed under the MATLAB/ Simulink environment. The curves obtained concerning the load voltage, the load current, the input current, and the curves of their FFT are given with and without compensation. In the last, the THD criterion is calculated.

Table 2 shows the parameters of the real three-phase source, the parameters of the MC, and those of the load.

The system's behavior without and with compensation is described by the results illustrated by Figs. 6 and 7, respectively.

Table 2
Parameters used for simulation.

Specifications		Values	
Input phase module	V_{im}	$220\sqrt{2}$	Volt
Average input frequency	F_{moy}	50	Hz
Variance of frequency	var	1	Hz
Instability time interval	$[t_1 t_2]$	$[0.01 0.07]$	S
Output frequency	F_o	50	Hz

Switching frequency	F_s	0.01	M.Hz
Modulation voltage ratio	q	0.75	
Resistive load	R_c	1	Ω
Inductive load	L_c	2	m.H

Figure 6 illustrates the behavior of the system without compensation: in (a), the input frequency is a random variable, which follows a normal distribution, its mean is 50 Hz, its variance is 1, its value changes every 0.001 s, and lasts for 0.01 s to 0.07 s; in (b), the wave shape of the voltage source is completely distorted; the frequency analysis in (c) reveals that undesirable frequencies are important; in (d), the current waveform deteriorates in $[t_1 t_2]$, and in (e) the frequency analysis of the current shows that the unwanted frequencies cover a range of 0 to about 400 Hz.

Figure 7 displays the system's behavior after using MC for compensation: in (a) the load voltage curve is good quality except for a few irregularities at the extremes. In (b), the load voltages (reference and obtained) are in phase, and the zero-crossing time is correct. In (c), the frequency analysis of the load voltage shows that the fundamental is remarkable, as we can distinguish harmonics of low value and no unwanted frequencies. In (d), the shape of the curves of the load current is of very good quality, which is in phase with its reference, and the zero crossing is respected in (e). In (f) The frequency analysis of load current presents the fundamental remarkably and an insignificant distortion. In (g) The input current curve is periodic and good quality except for a small deformation at 0.05 s. In (h) two frequencies are shown. The first is fundamental. The second is the third harmonic 150 Hz and no noise. The third harmonics is due to using the optimal Venturini method to increase the voltage gain q .

The THD is the last criterion used to determine the influence of harmonics on the effectiveness of this method. Only the first four harmonics are considered. The weight of each harmonic is calculated. The results obtained in percent are shown in Table 3.

Table 3
Calculated THD criterion

Frequency (Hz)	Load voltage		Load current		Input current	
	Before	After	Before	After	Before	After
150	2.56	1.65	2.36	0.03	2.36	13.39
250	4.20	1.32	0.22	0.10	0.22	0.55
350	5.85	0.75	1.34	0.00	1.34	0.31
THD	7.64	2.24	2.73	0.11	2.73	13.40

By comparing the results obtained before and after compensation, the THD of load voltage and load current decreased from 7.64 % to 2.24 % for the first and 2.73 % to 0.11 % for the second. They are acceptable. Therefore, the input current is high, from 2.73 % to 13.40 %. The harmonic two of 13.39 % is dominant, which is necessary to insert an adequate input filter.

The curves obtained in Fig. 7 and the THD calculations in Table 3 show that the system's behavior is well compensated except for the input current.

The disadvantage of this method is that at each instant of switching, the gain q is evaluated after 27 iterations of the calculation of the common function of Lyapunov as shown in equation 13, then the selection of which is the optimal choice. Thus, the number of operations carried out is very high compared to the fuzzy logic method in one iteration.

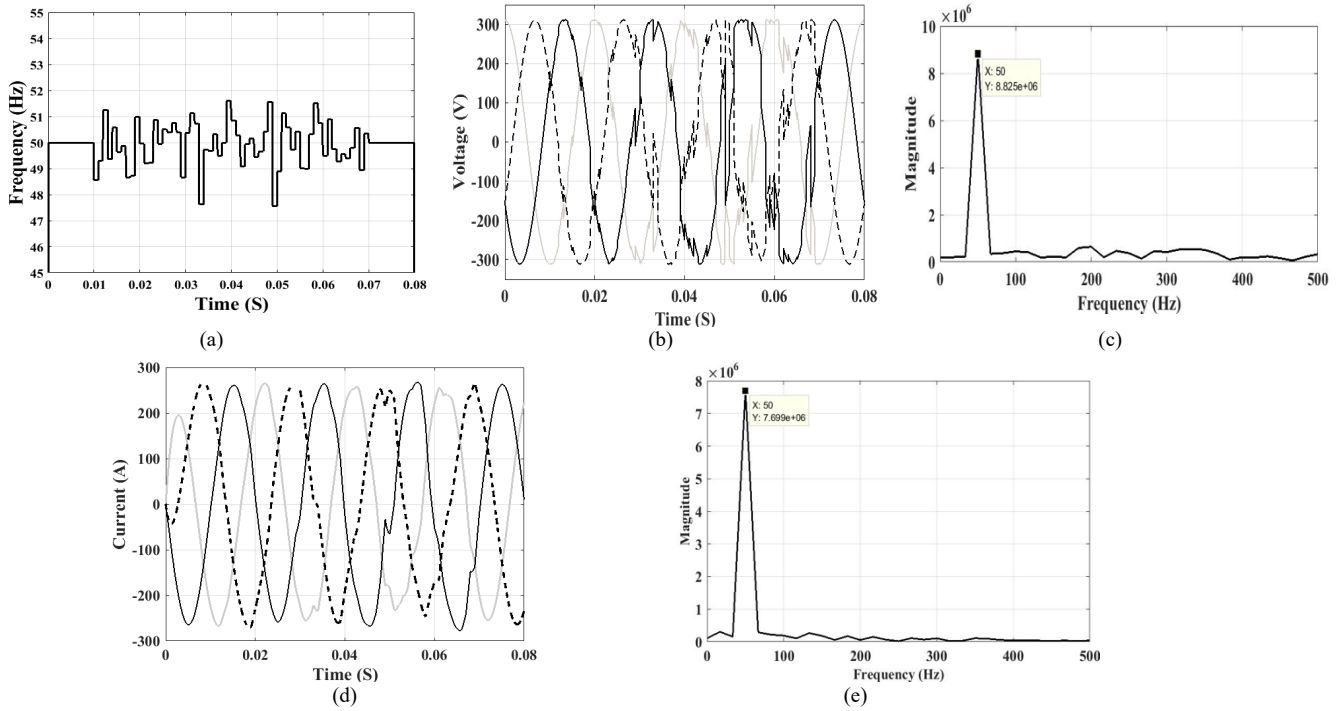


Fig. 6 – The behavior of the system without compensation: a) random input frequency; b) Input voltage; c) FFT of a phase of an input voltage; d) Current; e) FFT of a phase of an input current.

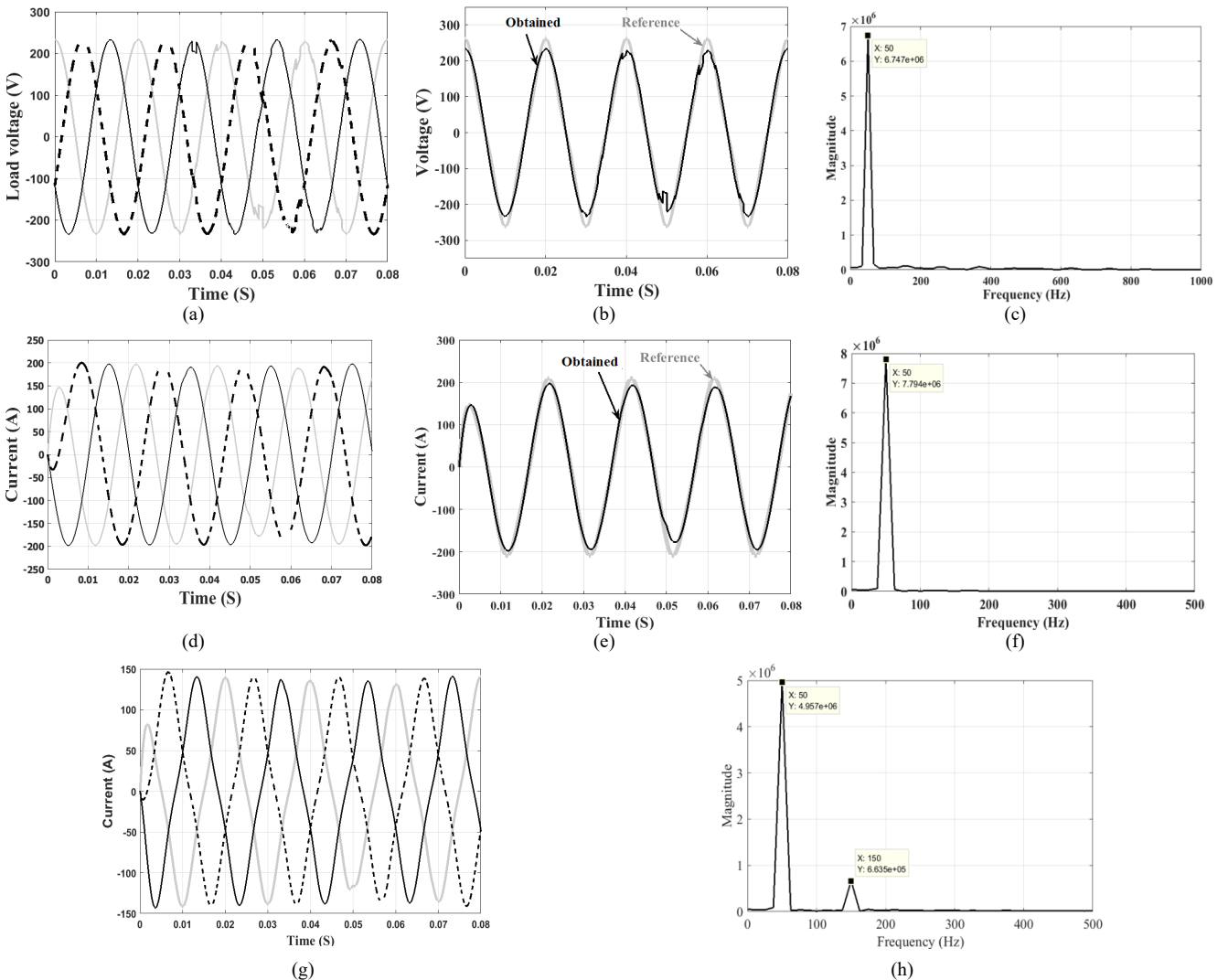


Fig. 7 – The behavior of the system after a compensation; a) load voltage ; b) load voltage (phase for a reference and obtained); c) FFT of load voltage; d) Load current; e) Load current (phase for a reference and obtained); f) FFT of a load current; g) input current; h) FFT of a phase of input current.

4. CONCLUSION

This article shows a new method for controlling an unstable energy source. It's based on the functions of Lyapunov, using an MC and the optimal amplitude method of Venturini.

The model is allowed only under ideal conditions. In this study, the frequency of the energy source is assumed to be unstable, and the distortion at the input of the MC is systematically transmitted to the output, which is the major inconvenience of the MC topology. To overcome this constraint, the contribution of the proposed approach is presented.

The study was conducted for a variable frequency energy source and a typical RL charge. The approach is simulated in the MATLAB/Simulink environment. The form of signals graph, the frequency analysis, thus, their THD are criteria used in the analysis.

According to the results, we conclude that this novel approach offers very significant performance.

Received on 1 August 2021

REFERENCES

1. L. Huber, D. Borojevic, *Space vector modulated three-phase to three-phase matrix converter with input power factor correction*, IEEE Transactions On Industry Applications, **31**, 6, pp. 1234–1246, 1995.
2. T.F. Podlesak, D.C. Katsis, P.W. Wheeler, J.C. Clare, L. Empringham, M. Bland, *A 150-kVA vector-controlled matrix converter induction motor drive*, IEEE Trans. Ind. Appl., **41**, 3, pp. 841–847, 2005.
3. A. Benyoussef, S. Barkat, *direct torque control based on space vector modulation with balancing strategy of dual star induction motor*, Rev. Roum. Sci. Techn.– Électrotechn. et Énerg., **67**, 1, pp. 15–20, Bucarest, 2022.
4. A. Dendouga, R. Abdessemed, M.L. Bendaas, *Active and reactive powers control of a doubly-fed induction generator fed by matrix converter*, E.P.E. Journal, **19**, 1, pp. 50–56, 2009.
5. L. Gyugyi, B.R. Pelly, *Static power frequency changers*. John Wiley & Sons, New York, NY, 1976.
6. M. Venturini, A. Alesina, *New sine wave in sine wave out, conversion technique which eliminates reactive elements*, Proc Powercon, 7, 3, pp 242–252, 1980. E3_1-E3_15
7. A. Alesina, M. Venturini, *Analysis and design of optimum-amplitude nine switch direct ac-ac converters*. IEEE Transaction. Power Electronics, **4**, 1, pp 101–112, 1989.
8. D. Casadei, G. Serra, A. Tani, *Reduction of the input current harmonic content in matrix converters under input/output unbalance*, IEEE Transactions on Industrial Electronics, **45**, 3, pp. 401–409, 1998.
9. H. Karaca, R. Akkaya, *A matrix converter controlled with the optimum amplitude-direct transfer function approach*, 6th International Conference On Electrical Engineering ICEENG, Cairo Egypt, 2008.
10. P.W. Wheeler, J. Rodriguez, J.C. Clare, L. Empringham, A. Weinstein, *Matrix converters: a technology review*, IEEE Trans. Ind. Electron, **49**, 2, pp. 276–288, 2002.
11. V. Veera, D. Pavel, J. Martin, B. Bedrich, *New modification of a single-phase ac-ac matrix converter with auxiliary resonant circuits for ac locomotives*, Rev. Roum. Sci. Techn.– Électrotechn. et Énerg., **61**, 1, pp. 73–77, Bucarest, 2016.
12. P. Patel, A. Mulla, *Space vector modulated three-phase to three-phase direct matrix converter*, IEEE. 16th International Conference on Environment and Electrical Engineering EEEIC, 7-10 June 2016.
13. J.J. Rodriguez, E. Peralta, O. Carranza, R. Ortega, *Optimal venturini modulation for a three-phase four-wire matrix converter*, IEEE Latin America Transactions, **14**, 2, pp. 617–623, 2016.
14. A. Boukadoum, T. Bahi, D. Dib, *Fuzzy logic control based matrix converter for improvement output current waveforms based wind turbine system*, International Journal of Renewable Energy Research, **3**, 3, pp. 586–591, 2013.
15. H. Chaoui, B. Hamane, M. Doumbia, *Adaptive control of Venturini modulation-based matrix converters using interval type-2 fuzzy sets*, J. Control Autom. Electr. Syst., **27**, pp. 132–143, 2016.
16. H. Karaca, R. Akkaya, *Modelling and simulation of matrix converter under distorted input voltage conditions*, Simulation Modelling Practice and Theory, **19**, 2, pp. 673–684, 2011.
17. M. Galea, G. Buticchi, L. Empringham, L. de Lillo, C. Gerada, *Design of a high force density tubular motor*, IEEE Trans. on Industry Applications, **50**, 4, pp. 2523–2532, 2014.
18. K. Khalil, *Nonlinear Systems*, Prentice Hall, 2001.
19. D. Liberzon, A. S. Morse, *Basic problems in stability and design of switched systems*, IEEE Control Systems Magazine, **19**, 5, pp. 59–70, 1999.
20. S. Pettersson, B. Lennartson, *LMI for stability and robustness of hybrid systems*, Proceedings of the 1997 American Control Conference, Albuquerque NM USA, 6 June 1997.
21. M.S. Braniky, *Multiple Lyapunov functions and other analysis tools for switched and hybrid systems*. IEEE Transactions on Automatic Control, **43**, 4, pp. 475–482, 1998.
22. R.A. Decarlo, M.S. Branicky, S. Pettersson, B. Lennartson, *Perspectives and results on the stability and stabilizability of hybrid systems*, Proceedings of the IEEE, **88**, 7, pp. 1069–1082, 2000.
23. V.F. Montagner, V.J.S. Leite, R.C.L.F. Olineira, P.L.D. Pers, *State feedback control of switched linear systems an LMI approach*, Journal of Computational and Applied Mathematics, **194**, 2, pp. 192–206, 2006.
24. A.V. Savkin, E. Skafidas, R.J. Evans, *Robust output feedback stabilizability via controller switching*, Automatica, **35**, 1, pp. 69–74, 1999.
25. G.S. Zhai, H. Lin, P.J. Antsaklis, *Quadratic stabilizability of switched linear systems with polytopic uncertainties*, Internat. J. Control, **76**, 7, pp. 747–753, 2003.